



# Influence of microstructure on adiabatic shear localization of pre-twisted tungsten heavy alloys

Zhigang Wei, Jilin Yu\*, Shisheng Hu, Yongchi Li

*Department of Modern Mechanics, University of Science and Technology of China, Hefei, Anhui 230027,  
People's Republic of China*

Received 4 August 1999; received in revised form 18 February 2000

---

## Abstract

The influence of microstructure of pre-twisted tungsten heavy alloy (WHA) on the adiabatic shear localization under dynamic loading was investigated experimentally. A combined compression and shear load was applied to a cylindrical specimen with its axis inclined to the loading axis by use of a split Hopkinson pressure bar (SHPB) apparatus which generates a strain rate as high as  $10^3 \text{ s}^{-1}$ . A relatively narrow shear band was formed approximately along the maximum shear stress direction, followed immediately by catastrophic fracture. Electronic microscopy and optical microscopy observations were made on the fracture surfaces and the microstructures of un-fractured specimens. It is found that the initial microstructures such as the aspect ratio and orientation of the W-grains have significant influence on the tendency to the shear band formation. The adiabatic shear band has general trends to propagate along the Ni–Fe matrix and more energy is needed to shear the tungsten grains. It is suggested that further studies on the optimization of microstructure and control of the fabricating process to promote the shear band formation be conducted in order to improve the penetration performance of the tungsten heavy alloy. © 2000 Elsevier Science Ltd. All rights reserved.

---

## 1. Introduction

Adiabatic shear localization is an especially important failure mechanism in structural impact. It is well known that the flow and failure behavior of a penetrator material strongly influences its penetration performance. Among kinetic energy penetrator materials, the ballistic performance of

---

\* Corresponding author. Tel.: 00-86-551-360-2179; fax: 00-86-551-363-7341.

E-mail address: jlyu@ustc.edu.cn (J. Yu).

most depleted uranium alloys (DU) is superior to that of the ordinary tungsten heavy alloys. Upon high-speed impact of a DU penetrator, adiabatic shear bands are formed at the edge of its head, along which cracks propagate. This “self-sharpening” effect reduces the diameter of the penetration tunnel, thereby improves the penetration performance [1]. However, the use of DU is restricted recently due to the environmental problems in all phases of application ranging from processing to battlefield cleanup. As an alternative, tungsten heavy alloy (WHA) is a potential candidate material for kinetic energy penetrators because of its low cost, high ductility and toughness, good ability in fabrication as well as high density and non-radioactivity. However, tungsten alloys were found to be insensitive to adiabatic shear failure. Hence, more of current studies are directed toward developing new types of the WHA that are more effective on the battlefield through controlling its microstructure to promote shear band formation [2].

Recently, it is aware that pre-twisted WHA projectiles show better ballistic performance than that of the ordinary untwisted ones. The diameter of the penetration tunnel as well as the ballistic limit of pre-twisted WHA penetrators were effectively reduced [3]. The reason of the improved penetration performance can be attributed to the “self-sharpening” effect. However, like untwisted tungsten alloy, pre-twisted tungsten alloy is also insensitive to adiabatic shear failure under uniaxial compression condition. Adiabatic shear band was not observed in our previous uniaxial impact tests using the SHPB apparatus at high strain rates, though deformation localization within the matrix occurs in pre-twisted tungsten heavy alloys [3].

In order to improve the ballistic performance of pre-twisted tungsten heavy alloy penetrators, it is essential to investigate the mechanism of the “self-sharpening” effect of the penetrators at high velocity impact. The influence of the microstructure, such as heterogeneity, the content of the matrix and the particle shape, on shear band formation was reported by Bose et al. [2] and Kim et al. [4]. Pressure/shear plate-impact experiments have shown that two-phase composite is more susceptible to the formation of shear band than either of its constituents [5,6]. Finite element simulations was conducted by Batra et al. [7,8] to simulate the formation of adiabatic shear band where the WHA alloy was modeled as a tungsten matrix with randomly distributed Fe–Ni–W particles. The behavior of tungsten composites at high strain rates has also been analyzed by other investigators [9–13].

In fact, the head of a penetrator is in a three-dimensional stress condition. Hence it is worthy of further investigation into the behavior of pre-twisted tungsten heavy alloy under more complex stress states, especially the influence of its microstructure on the adiabatic shear band formation. It is hoped that such investigation will provide an insight into the way to improve the ballistic performance of the WHA penetrators through alloy design, fabrication process and microstructure optimization.

It is the intent of this paper to provide a description directed toward a coherent understanding of the sensitivity of the adiabatic shear localization to the microstructure parameters, such as the shape and the orientations of the W-grains. A combined compression/shear testing method proposed by Meyer [14] was employed in the SHPB apparatus to promote adiabatic shear localization [15]. The deformed microstructures were examined with the scanning electron microscopy and the optical microscopy respectively. Adiabatic shear localization has been observed in our high strain-rate compression/shear tests.

## 2. Experimental setup

The W–Ni–Fe heavy alloy used in this work contains 93% of tungsten by weight with a nickel-to-iron ratio of 7 : 3. The alloy was manufactured by liquid-phase sintering of the blended elemental powders, followed by vacuum annealing for several hours. Some of the WHA rods were twisted quasi-statically by a torsion machine. Then, specimens were made of both untwisted and pre-twisted rods for dynamic tests. The specimens were machined that the normal of the two end surfaces is inclined to its longitudinal axes with various inclinations, i.e.  $10^\circ$ ,  $20^\circ$  and  $30^\circ$ , respectively. The microstructure of the original untwisted tungsten alloy consists of spherical tungsten grains (typically 30–60  $\mu\text{m}$  in diameter) surrounded by Ni–Fe matrix, as shown in Fig. 1. The microstructure of the pre-twisted WHA is shown in Fig. 2 where the axis of the rod is vertical. It can be seen that originally spherical W-grains have been deformed to an ellipsoidal shape due to torsion. The aspect ratio of the tungsten grains is about 1.8.

A split Hopkinson pressure bar is used to load samples at strain rates of  $10^2$ – $10^4 \text{ s}^{-1}$ . A schematic drawing of the apparatus is shown in Fig. 3, which is essentially the same as that described by

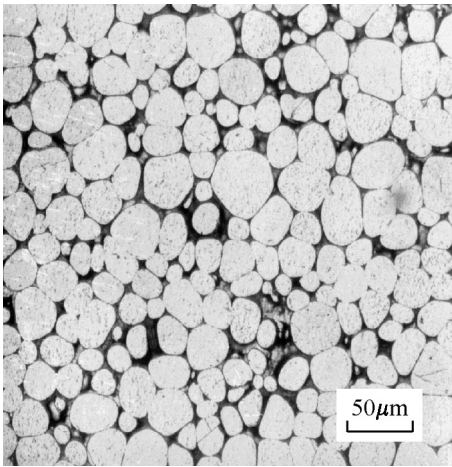


Fig. 1. Microstructure of the initial untwisted WHA.

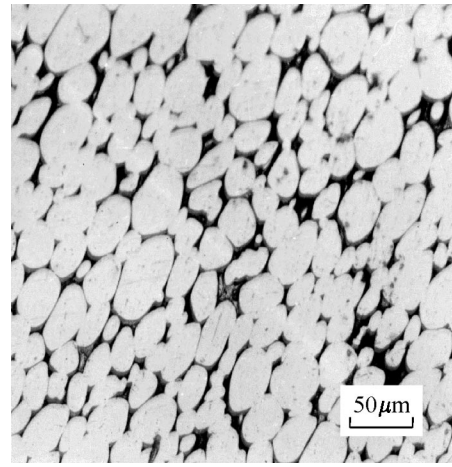


Fig. 2. Microstructure of a pre-twisted WHA.

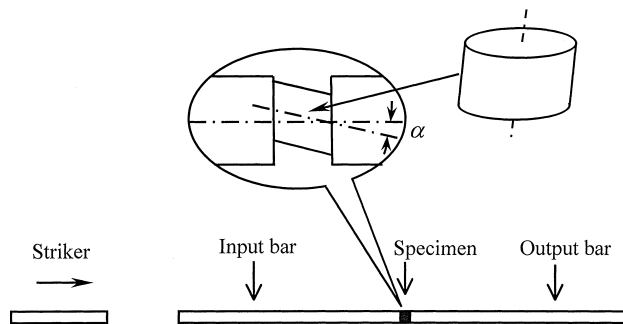


Fig. 3. Sketch of the split Hopkinson pressure bar setup.

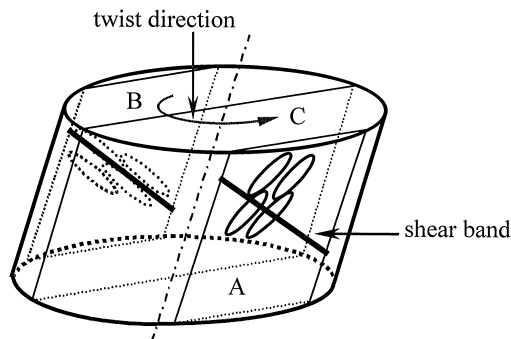


Fig. 4. Schematic description of the orientation of W-grains and adiabatic shear band and the sections of microstructure observation.

Lindholm [16]. The device consists of two long elastic bars, between which a small inclined cylindrical specimen is sandwiched. A projectile fired from the gas gun strikes the incident bar and generates a compressive stress wave that propagates into the specimen. Both reflected and transmitted stress waves are recorded by strain gages placed on the incident and transmitted bars, respectively.

Assuming the specimen deforms in a uniform stress state, the strain gage signals can be used to calculate the histories of the strain rate and the stress of the specimen in the longitudinal direction of the apparatus. The longitudinal strain history is then obtained by integrating the strain rate.

Scanning electron microscope studies are performed on the fractured specimens after tests in order to identify fracture characteristics and its mechanism. Some un-fractured specimens are precisely cut along surfaces parallel to the axial direction, as shown in Fig. 4, and polished and etched. Then, these sections are characterized using the optical microscopy to examine the deformation and fracture behavior of the specimen.

### 3. Results

#### 3.1. Fractured specimen

Fig. 5 shows schematic drawings of the failure procedure of the specimens, and Fig. 6 is a photograph of a fractured specimen. Macroscopic fracture developed along the minor diagonal (similar to that described in Ref. [14]). Surface D was formed due to the subsequent compressive loading after specimen fracture during the test. Not losing the generality, we will concentrate our efforts to investigate specimens with a typical inclination angle of  $10^\circ$ , though there are some differences between the results of specimens with different inclination angles, which are similar to that described by Meyer [14].

The fracture surfaces of the ruptured specimens were examined using a scanning electron microscope to investigate the deformation and fracture mode involved in the dynamic compression/shear tests. Fig. 7(a)–(c) show fractographs of the rupture surface at different positions, points

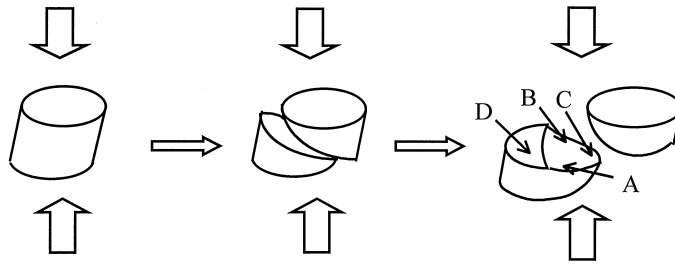


Fig. 5. Fracture procedure of an inclined specimen.



Fig. 6. Photograph of a broken specimen under dynamic compression/shear loading.

A, B and C in Fig. 5, respectively.<sup>1</sup> It is observed that the fracture surfaces at points A, B and C contrast dramatically. The surface at point C is much smoother than that at points A and B. It is difficult to distinguish the tungsten grain from the matrix in Fig. 7(c). The reason is that point C was smeared for a longer time than points A and B due to rubbing of the fracture surfaces during the failure process. The main feature of Fig. 7(a) is a periodically coarse surface indicating the rupture of highly deformed W-grains. The deformation and fracture process seems to be dominated mainly by tungsten grains, and the role of the matrix is minor. In contrast, in Fig. 7(b) the remaining half of the fractured W-grain at point 1, the tungsten grain-matrix separation at point 2, W–W separation at point 3, and the ductile matrix rupture are evident. Elliptic tungsten grains can be seen clearly on the surface, indicating the deformation of tungsten grains is evidently smaller than that in Fig. 7(a). All these results provide evidences that a combination of ductile rupture of matrix, grain-matrix separation, W–W separation and W-grain brittle fracture is responsible for the failure at point B.

<sup>1</sup> Positions A, B, C in Fig. 5 correspond to those in Fig. 4. However, Figs. 4, 8–10 are for the un-fractured specimen and observations are made on surfaces parallel to the axial direction, while Figs. 5 and 7 are for the fractured specimen and observations are made on the fractured surface.

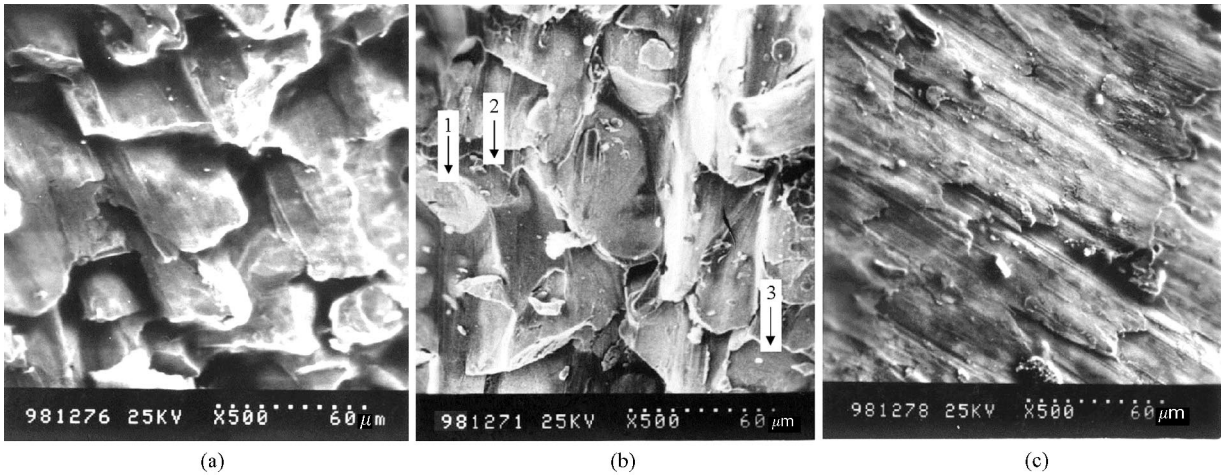


Fig. 7. Fractographs of the rupture surface at different positions: (a) point A, (b) point B, and (c) point C.

### 3.2. Un-fractured specimen

To further investigate the deformation behavior and the microstructural influence on the adiabatic shear localization, some impact tests with lower kinetic energy were conducted. These specimens were not broken. Inhomogeneous deformation is not observed by visual inspection. However, adiabatic shear localization within these specimens is observed by the optical microscope. A schematic description of the observation sections of a typical specimen is shown in Fig. 4.

Fig. 8 shows the micrographs of a narrow shear band at one side of the specimen, on section A in Fig. 4. Here the direction of the maximum shear stress crosses the direction of the major axis of

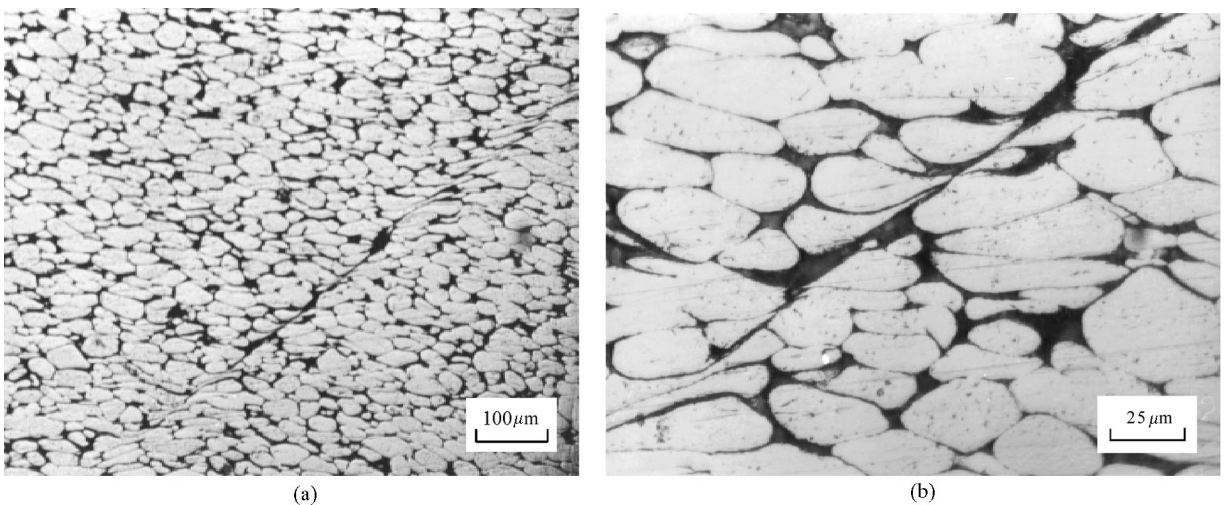


Fig. 8. Micrographs of a narrow shear band at one side of the specimen, on section A.

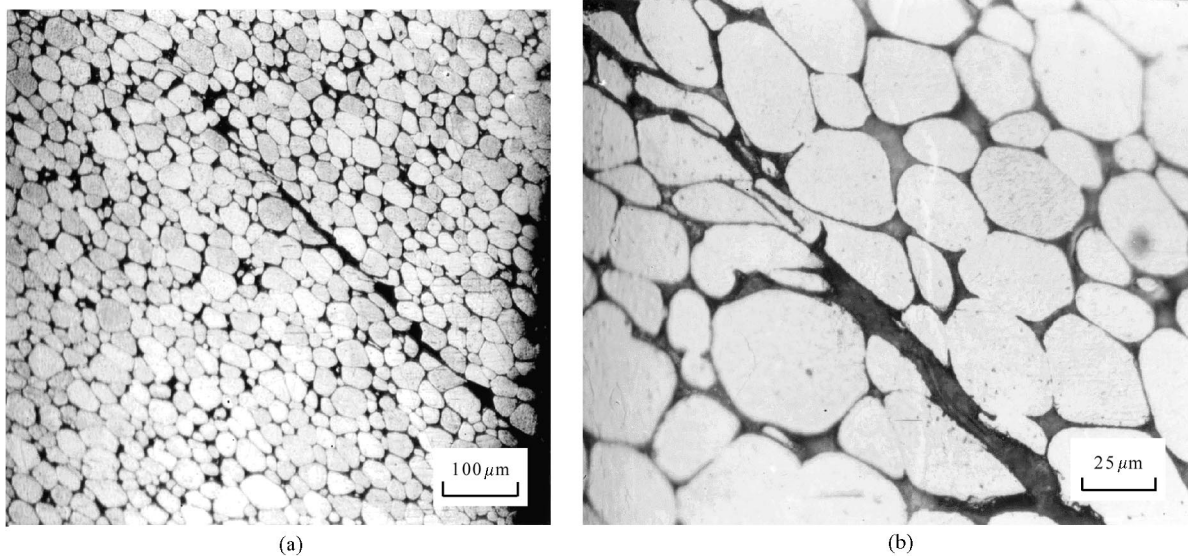


Fig. 9. Micrographs of a shear crack at the other side of the specimen, on section B.

tungsten grains with a large angle. Significantly elongated tungsten grains in the middle of the specimen indicate a developing adiabatic shear band. The W grains were elongated and some of them were subsequently ruptured into two teardrops near the middle of the band. This result is consistent with that shown in Fig. 7(a). Away from the center of the shear band, tungsten grains were largely deformed. It transpires that tungsten grains endure mostly the deformation due to compression before the shear band formed.

Fig. 9 shows the micrographs at the other side of the specimen, section B in Fig. 4, with a narrow shear crack. The direction of the maximum shear stress there is approximately parallel to the direction of the major axis of tungsten grains. Away from the crack, tungsten grains were rarely deformed. Most of the deformation seems to be concentrated in the matrix. It can be seen that tungsten grains endure less deformation than in Fig. 8. The crack was formed in tungsten grains, indicating a brittle feature of the tungsten. This is in accord with the SEM observation shown in Fig. 7(b).

At the central section, on section C in Fig. 4, a typical shear band was formed from the edge of the inclined specimen and propagated into the bulk along the minor diagonal, as shown in Fig. 10. Near the shear band the grains were highly distorted and elongated. It should be noted that in the specimen only one shear band was formed and propagated along a direction with almost linear pattern. The shear band here appears to involve the tungsten grains as well as the matrix. Within the band the tungsten grains were heavily deformed, and pulled into long stringers along the shear direction. This is in accord with the characteristics described in Fig. 7(c). Away from the center of the shear band by about 50  $\mu\text{m}$ , tungsten grains are rarely deformed. It can be seen that tungsten grains endure rarely deformation due to the compression before the shear band formed. The width of the shear band is less than 100  $\mu\text{m}$  and the maximum shear strain within the band is over 1000%. Away from the shear band the tungsten grains were able to rotate themselves sufficiently to accommodate the shear deformation.

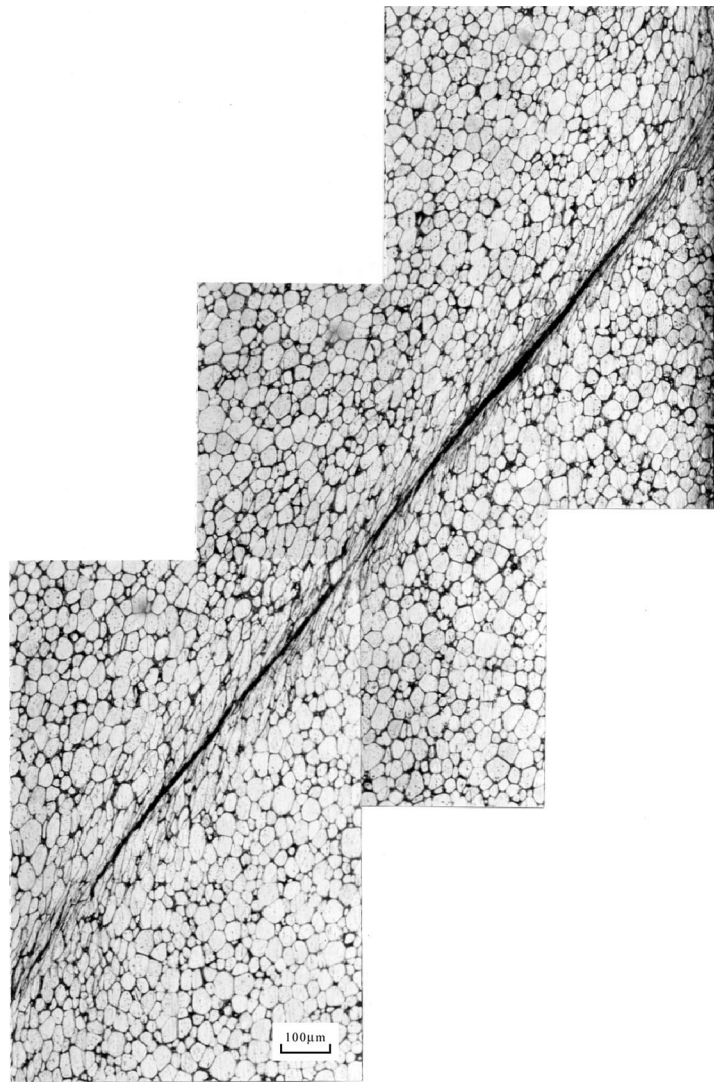


Fig. 10. Micrographs of a shear band at the central section, section C.

In view of the high percentage of the W-grain supra-ductile fracture in shear band shown in Fig. 8, adiabatic shear deformation and fracture of W-grains appears to be the dominant mechanism in this side of the specimen. Here the direction of the maximum shear stress cross the direction of the major axis of tungsten grains with a large angle. In the other side of the specimen, the direction of the maximum shear stress is approximately parallel to the direction of the major axis of tungsten grains. A combination of ductile rupture of matrix, grain-matrix separation, W–W separation and W-grain brittle fracture appears to be responsible for the failure of the pre-twisted WHA. All these results indicate that the shape and the orientation of the tungsten grains have



significant influence on the formation of adiabatic shear band and cracks in the pre-twisted tungsten alloy.

#### 4. Discussion

The Ni–Fe matrix is known to be significantly weaker than the tungsten grains. Its flow stress is only approximately one half of that of the pure tungsten. Hence the shear deformation in the dual-phase material is essentially controlled by the deformation of the weak phase, i.e. the matrix.

During a dynamic deformation process, initially most of the plastic deformation will occur in the matrix. It will be strained and work-hardened, and then softened due to a rapid temperature rise by plastic work. Melting is likely to occur because the melting point of the matrix is low. Zurek and Follansbee [17] have shown that thermal-mechanical behaviors can strongly effect the formation of adiabatic shear band. In fact, iron is sensitive to adiabatic shear localization [18]. Experiments show that large pools of matrix materials tend to favor the process of shear localization [2]. In comparison, tungsten shows a much lower rate of thermal softening than that of the matrix, partly because of its less plastic deformation and high melting temperature (approximately 3300 K, versus 1750 K for the matrix). Adiabatic shear band in pure tungsten has never been found, while adiabatic shear localization in tungsten grains were observed in a combined compression/shear condition. However, more energy is needed for shear deformation in tungsten grains than in matrix. Interfaces between tungsten grains also have a brittle nature and work as deterrents for the shear band formation and propagation [19,20].

It should be noted that Ramesh and Coates [21] reported somewhat different effects of tungsten and matrix of similar materials. They concluded that the matrix material has negligible effect on compressive deformation at significantly large strains, though during the early stages deformation occurs mainly in the matrix. However, it is worth to point out that their tests were in uniaxial compression where shear deformation is unlikely to occur. Adiabatic shear localization is sensitive to stress condition. When a specimen is under dynamic uniaxial compression, there is no favorite direction of shear deformation. Hence adiabatic shear band is hardly found in the tungsten heavy alloy under uniaxial compression condition. However, for a specimen under compression/shear loading, shear band localization may take place along the maximum shear direction.

It is interesting to notice that the deformation and failure mechanisms are very different at points A and B in Fig. 5, although the macroscopic conditions at the two positions are approximately identical.<sup>2</sup> This phenomenon indicates a strong influence of the microstructure on the shear localization for dual-phase materials.

Generally speaking, for dual phase materials such as WHA, the matrix favors the initiation of shear localization. However, due to the resistance of the tungsten grains, the tendency of shear band formation and growth becomes lessened. For pre-twisted WHA with elongated tungsten grains, in comparison with untwisted WHA, shear band is easier to propagate mainly within the matrix in the region where the major axis of the grains parallels to the maximum shear stress

---

<sup>2</sup> Due to the pre-twist, specimen material will exhibit slight anisotropy, which is not uniformly distributed. As a consequence, the macroscopic conditions at A and B are somewhat different. But the influence is not significant.

direction. The tendency of shear band formation increases. Once a shear band initiates in the matrix, the resistance to the applied load is radically reduced, leading to an unstable process of the propagation of shear band and subsequent crack propagation in the matrix. Eventually, the “self-sharpening” effect occurs.

When a pre-twisted WHA specimen is under compression/shear loading, the direction of maximum shear stress is parallel to the minor diagonal of the specimen. At one side of the specimen, the direction of the maximum shear stress is approximately parallel to the direction of the major axis of tungsten grains. Shear localization in the matrix there is easier for it is less deterred by tungsten grains. The nearby tungsten grains might be softened due to the heat conduction from the heavily deformed matrix and localized deformation forms in tungsten grains near the tungsten-matrix interfaces. In addition, the material there has undergone plastic shear deformation in the same direction during the pre-twist process. Presumably less energy is needed to form an adiabatic shear band in the WHA through this mechanism. At the other side, the direction of the maximum shear stress crosses the direction of the major axis of tungsten grains with a large angle. Shear band localization in the matrix is impossible but, in comparison with untwisted tungsten grains, tungsten grains there are easier to be sheared across the minor axis due to its shape as well as the work hardening during pre-twist process, though the energy required by this mechanism is higher than that on the other side. Presumably shear band localization will first occur at the side where shear deformation within the matrix is easier. Then, due to the loss of load-bearing capacity there, adiabatic shear band will develop at the other side. This is in agreement with the different stages of the failure process at the corresponding positions shown in Figs. 8–10.

From the above analysis, it can be seen that the influence of microstructure on the adiabatic shear band formation is substantial. It is expected that proper change of the microstructure such as the aspect ratio, the grain orientation, the strength of the tungsten-matrix interface, etc. will improve the “self-sharpening” effect and ballistic performance of tungsten heavy alloy penetrators.

In order to obtain quantitative estimation of the effect of pre-twist on the sensitivity of the adiabatic shear band formation, detailed analysis of the stress and strain states in the test specimen is necessary. Further experimental investigation and numerical simulation are under consideration.

## **5. Conclusions**

Combined dynamic compression/shear tests were conducted to study the deformation and failure behavior of pre-twisted tungsten alloy at high strain rates. The following conclusions can be drawn from the results.

1. Adiabatic shearing localization, followed immediately by catastrophic fracture, has been observed in pre-twisted tungsten heavy alloy at the high rate compression/shear tests.
2. The rupture of W-grain (adiabatic shear) is the dominant failure mechanism at one side of the pre-twisted WHA, where the direction of the maximum shear stress cross the direction of the major axis of tungsten grains with a large angle. On the other hand, a combination of ductile rupture of matrix, grain-matrix separation, W–W separation and W-grain brittle fracture is the failure mechanism at the other side of the specimen, where the direction of the maximum shear stress approximately parallel to the direction of the major axis of tungsten grains.

3. Presumably the adiabatic shear band initiates at one side where the direction of the maximum shear stress approximately parallel to the direction of the major axis of tungsten grains, and then develops at the other side due to the loss of load-bearing capacity.

4. The shape and the orientation of the W-grains play an important role in the formation of adiabatic shear band in the pre-twisted tungsten alloy specimens. Plastic deformation during the pre-twist process may also contribute to the susceptibility of the specimen to the shear band formation.

## Acknowledgements

This work is supported by the National Natural Science Foundation of China (project No. 19672060) and the Chinese Academy of Sciences (major research project No. KJ951-1-201).

## References

- [1] Magness LS. Properties and performance of KE penetrator materials. In: Bose A, Dowding RJ, editors. Proceedings of the First International Conference on Tungsten and Tungsten Alloys, Arlington VA, November 15–18, Metal Powder Industries Federation. 1992. p. 15–22.
- [2] Bose A, Congue H, Lankford Jr J. Influence of microstructure on shear localization in tungsten heavy alloys. In: Bose A, Dowding RJ, editors. Proceedings of the First International Conference on Tungsten and Tungsten Alloys, Arlington VA, November 15–18, Metal Powder Industries Federation. 1992. p. 291–8.
- [3] Wei ZG, Hu SS, Li YC, Fan CS. Dynamic properties and ballistic performance of pre-torqued tungsten heavy alloys. In: Niekerk CV, editor. Proceeding of the 17th International Symposium on Ballistics, vol 3. South Africa: The South Africa Ballistics Organization. 1998. p. 391–398.
- [4] Kim DK, Lee S, Song HS. Effect of tungsten particle shape on dynamic deformation and fracture behavior of tungsten heavy alloys. *Metall Mater Trans A* 1998;29:1057–69.
- [5] Zhou M, Needleman A, Clifton RJ. Finite element simulations of dynamic shear localization. *J Mech Phys Solids* 1994;42:423–58.
- [6] Zhou M, Clifton RJ. Dynamic constitutive and failure behavior of a two-phase tungsten composite. *J Appl Mech* 1997;64:487–94.
- [7] Batra RC, Wilson NM. Adiabatic shear bands in plane strain deformations of a WHA. *Int J Plasticity* 1998;14:43–60.
- [8] Stevens JB, Batra RC. Adiabatic shear bands in the Taylor impact test for a WHA rod. *Int J Plasticity* 1998;14:841–54.
- [9] Baek WH, Hong MH, Lee S, Chung DT. A study of the shear localization behavior of tungsten heavy alloys. In: Bose A, Dowding R, editors. Proceedings of the 2nd International Conference on Tungsten and Refractory Metals: Mclean, VA, 1994. p. 463–71.
- [10] Tham RH, Hohler V. Dynamic behavior of novel tungsten penetrator materials. In: Bose A, Dowding R, editors. Proceedings of the 2nd International Conference on Tungsten and Refractory Metals: Mclean, VA, 1994. p. 159–66.
- [11] Woodward RL, Alkemade SJ, Magness LS. Strain localization and fracture in dynamic dumbbell compression of tungsten alloy. In: Bose A, Dowding R, editors. Proceedings of the 2nd International Conference on Tungsten and Refractory Metals, Mclean, VA, 1994. p. 431–45.
- [12] Yadav S, Ramesh KT. The mechanical properties of tungsten-based composites at very high strain rates. *Mater Sci Engng* 1995;A 203:140–53.
- [13] Zhao D, Vailencia JJ, McCabe TJ. Mechanical and microstructural behavior of tungsten heavy alloys during high rates deformation. In: Bose A, Dowding R, editors. Proceedings of the 3rd International Conference on Tungsten and Refractory Metals: Mclean, VA, 1995. p. 123–30.

- [14] Meyer LW, Staskewitsch E, Burbli A. Adiabatic shear failure under biaxial dynamic compression/shear loading. *Mech Mater* 1994;17:203–14.
- [15] Wei ZG, Hu SS, Yu JL, Li YC. Adiabatic shear localization of pre-twisted tungsten heavy alloys under dynamic compression/shear loading. In: Shim VPW, Tanimura S, Lim CT, editors. *Impact response of materials and structures*. Oxford: Oxford University Press, 1999. p. 178–83.
- [16] Lindholm US. Some experiments with the split Hopkinson pressure bar. *J Mech Phys Solids* 1964;12:317–35.
- [17] Zurek AK, Follansbee PS. A comparison of shear localization susceptibility in U-0.75 Wt pct Ti and W-Ni-Fe during high strain rate deformation. *Metall Mater Trans A* 1992;26:1483–90.
- [18] Bai Y, Dodd B. *Adiabatic shear localization*. New York: Pergamon, 1992.
- [19] Kim DK, Lee S, Baek WH. Microstructural study of adiabatic shear bands formed by high-speed impact in a tungsten heavy alloy penetrator. *Mater Sci Engng A* 1998;249:197–205.
- [20] Kim DK, Lee S, Noh JW. Dynamic and quasi-static torsional behavior of tungsten heavy alloy specimens fabricated through sintering, heat-treatment, swaging and aging. *Mater Sci Engng A* 1998;247:285–94.
- [21] Ramesh KT, Coates RS. Microstructural influence on the dynamic response of tungsten heavy alloys. *Metall Mater Trans A* 1992;23:2625–30.